

# Projecting Emotions through Aquatic Interactions and the Creation of a Water-Propulsion Robot

Sarah T Tan

CMU-RI-TR-17-70

December 2017



The Robotics Institute  
School of Computer Science  
Carnegie Mellon University  
Pittsburgh, PA 15213

**Thesis Committee:**

Aaron Steinfeld, Advisor

Michael Kaess

Ellen Cappelletti

*Submitted in partial fulfillment of the requirements  
for the degree of Master of Science in Robotics.*

Copyright © 2017 Sarah T Tan

**Keywords:** Underactuated controls, Water-jet nozzles, Fluid mechanics and applications, Basic motion, Movement-based emotions, Water-propulsion robots

## **Abstract**

Expressing robot intent through movements is a key factor in the acceptability of new robotic systems. One way to express intent is to connect communication and emotions. The concept of generating motions to portray a body language can aid in the speed of communication between humans and robots. However, body language and expressibility can be heavily influenced by the situated environment.

In this thesis, we investigate the creation of a new robotic system with a unique aquatic environment to generalize the connection between portraying emotions and robotic system movements, using water as an aid in the communication. Through the creation of this innovative aquatic robot platform, we produce a unique set of behaviors and responses that impart environmental changes such as water spray, splashes, and bubbles. In addition, we will delve into the development and assessment of various movement patterns and the expression of emotions.



## **Acknowledgments**

Firstly, thanks to Prof. Aaron Steinfeld for having faith in my research interest and direction. The guidance that Aaron has provided me, for nearly 2 years now, has proved invaluable and has allowed me to visibly grow.

Thank you to all of my labmates and classmates who have worked alongside me. Specifically, I wish to acknowledge Marynel Vazquez for providing support, valuable contacts and information, and giving her time to meet with me. Furthermore, I would like to thank Ellen Cappo and Stelian Coros for providing me with valuable support and guidance directly toward my thesis. In addition, thanks to Ellen, I was truly able to understand the controls of the system. Lastly, I'd like to thank Prof. Michael Kaess for his incredible interest, insight, and support in the direction of my thesis and creation of my water-propulsion system.

Also, thanks to all of the professors and friends that supported me throughout my academic career.



# Contents

<b>1</b>	<b>Introduction</b>	<b>1</b>
1.1	Prior Work . . . . .	2
1.1.1	Water Propulsion . . . . .	2
1.1.2	Quadcopter Control . . . . .	3
1.1.3	Encoding Emotions . . . . .	3
1.2	Thesis Problem . . . . .	4
1.3	Contribution and Outline . . . . .	4
<b>2</b>	<b>Overall Design</b>	<b>7</b>
2.1	Design of Mechanical Structure . . . . .	7
2.1.1	Overall Mechanical System Architecture . . . . .	7
2.1.2	Low-Center of Gravity Disk . . . . .	9
2.2	Design of the Electrical System . . . . .	9
2.2.1	Overall Electrical System Architecture . . . . .	10
2.3	Discussion . . . . .	10
<b>3</b>	<b>Water-Propulsion System</b>	<b>13</b>
3.1	Water Jet Nozzle Design . . . . .	13
3.1.1	Nozzle Shape . . . . .	13
3.1.2	Generated Thrust . . . . .	14
3.1.3	Efficiency Comparison of Nozzle Shape . . . . .	17
3.2	Software System Architecture . . . . .	18
3.2.1	Control Algorithms . . . . .	18
3.3	Discussion . . . . .	19
<b>4</b>	<b>Expression of Emotions from Motion Profiles</b>	<b>23</b>
4.1	Creation of Motion Profiles . . . . .	24
4.2	Resulting Motion Behaviors . . . . .	25
4.2.1	Happy Behavior . . . . .	25
4.2.2	Shy Behavior . . . . .	25
4.3	Discussion . . . . .	26
<b>5</b>	<b>Conclusion</b>	<b>29</b>
5.1	Summary . . . . .	29
5.2	Limitations . . . . .	30
5.3	Future Work . . . . .	30



# List of Figures

- 1.1 Lin et al. [23] Spherical Underwater Water-Jet Robot (left) and Jetlev-Flyer (right) . . . . . 3
- 1.2 Quadcopter dynamics image detailing the different motions quadcopters can have and exert [31] . . . . . 4
- 2.1 Created and Designed CAD model and prototype of *Firefly*. . . . . 8
- 2.2 CAD drawing of a potential gimbal system to work onboard *Firefly* using waterproof servo motors with roughly 120oz-in of torque. . . . . 8
- 2.3 Free body diagram detailing the equations of motion for *Firefly* . . . . . 9
- 2.4 Electrical architecture diagram detailing the communication method and power distribution. 10
- 3.1 Taken from [29], nozzle exit orifices and the relationship to the coefficient of discharge  $C_d$  to maximize efficiency of flow. . . . . 14
- 3.2 Prototype water-propulsion nozzle design for *Firefly*. . . . . 15
- 3.3 Thrust testing setup to measure the grams of force produced by a nozzle’s propulsion. Nozzle is installed in the red box and measurements were read within the blue box. Nozzle force is converted into grams of thrust on the scale rotating on a single axle. . . . . 15
- 3.4 Experimentally determined relationship between thrust and inlet pressure on 1.5mm and 2.0mm nozzles with 8 – 10 measurements. . . . . 16
- 3.5 Experimentally determined relationship between thrust, valve opening, and inlet pressure on a 2.0mm nozzle with 102 measurements. . . . . 17
- 3.6 Software system architecture block diagram detailing the communication scheme between sensors, motors, and the main control loop and system state . . . . . 19
- 3.7 There are three major PID loops which control the stability and altitude of the robot. The jet  $i$  position  $x_i$  is adjusted with each corresponding PID, ultimately resulting in  $\delta x_i$  for the final adjusted jet position which is then commanded to the motors. . . . . 20
- 3.8 The neural network architecture was used to better approximate the correlation between a sensory input space of over 12 features to the best predicted jet nozzle opening for each of the four jets. Activation layers of sizes 8 and 6 were used as the internal components of the neural network. . . . . 20
- 4.1 Water effects using FlyBoard as part of a water show [8]. . . . . 23
- 4.2 Taken from [13], interaction profiles are detailed using Interaction Vocabulary [21]. On the left, the encoding for grumpy (red) and shy (green) profiles are shown. On the right, the encoding for happy (blue) and brave (green) are shown. These drone-interaction profiles were developed by Cauchard et al. through a 5-person study assigning stereotypes of personality to Interaction Vocabulary characteristics. . . . . 24

- 4.3 Storyboard of happy behavior movement through time steps. *Firefly* rapidly hops toward and approaches the interaction object (rubber ducks) from multiple angles. The robot always stays within close proximity of the ducks and occasionally bumps the ducks. . . . 26
- 4.4 Storyboard of shy behavior movement through time steps. *Firefly* slowly approaches the interaction object (rubber ducks) from multiple angles. The robot always keeps distance between the ducks and never physically bumps the ducks. Additionally, *Firefly* will rapidly hops or moves away from the ducks after some amount of time approaching them. . . . 26

# List of Tables

- 3.1 Comparison between tube diameter with no nozzle (6.35mm), 1.5mm, and 2mm nozzles on average experimentally generated inlet pressure, elapsed time, mass flow rate, velocity, and thrust. . . . . 16
- 3.2 Comparison using the coefficient of discharge between the constructed and ideal nozzle shape for both straight edge and radius lead orifices. . . . . 18
- 4.1 Description of Interaction Vocabulary created with reference to [21] regarding *Firefly* and its movement patterns. . . . . 24



# Chapter 1

## Introduction

Eliciting emotions and portraying a body language that can be perceived in social interactions are becoming increasingly important for robots as they become more intertwined in the daily lives of people globally. Currently, robots found in social settings are required to communicate and cooperate with humans either through symbols, signs, or languages [26]. However, communicating with these methods can be inefficient and challenging because either static visuals or verbal communication are required between person and robot; robots indicate conditions through screens and sounds.

If robots, however, could form a body language of intentions based on movements, the time taken for human-robot interactions can decrease. Rather than requiring a person to look at a diagnostic monitor and/or spend time verbally communicating, robots could portray indicators while still performing tasks. For example, robots might indicate low batteries through sleepy and slow movements or they might indicate malfunctions and danger through sporadic and sudden changes in behavior [10]. Additionally, these kinds of alterations in expected motions could pose useful for both robot maintenance and diagnostics while creating a safer workspace for humans.

Not only do the patterns and speeds of movements affect the portrayal of intent and emotions, but the changes in environmental interactions can also vary the portrayal. Some robots, such as Shimon and Travis [17], are specifically built and designed to express emotions through gestures on stationary bases. However, most robots are not designed and situated solely for emotional expressibility. Instead, robots are typically limited by the degrees of freedom, joint limits, and operating environments. Therefore, rather than having specific predefined gestures to portray intent, another approach might be to incorporate interaction characteristics into each motion.

In particular, this thesis focuses on using movement on and through an aquatic medium to portray emotion characteristics. Motion behaviors on water are generated by a unique four-jet robot which uses water-propulsion as an additional medium to express emotions.

Currently, there has been little investigation between aquatic environments and robot interactions. However, moving water is a distinct and visible show component which can aid in the expressibility of a robot. In addition, using an aquatic medium allows for unexpected motions such as buoyancy on a robot, bubbles, and water splashes. Thus, to incorporate both the effect of water and the additional factors from operating in an aquatic medium, the robot was created to use water-propulsion as both the movement and emotional expressibility mechanism.

The most prominent works involving robots and water-propulsion centralize on performing tasks such as water-jet cutting. However, there are a few water-propelled robots comprising of underwater vehicles and above-water jet packs [3, 22, 23]. Using a water-propulsion system in aquatic environments can help decrease the number of variables for motion control and create a more predictable movement. In particular,

for tasks such as firefighting or washing boats, there is both a use case for water-jets to put out fires or shoot a jet stream at a boat respectively, in addition to using water-jets as the method for motion. As shown by above-water jet packs [3], however, the concept of water-propulsion can be used as a form of travel through different aquatic mediums - a system could be created which could travel below, through/on, and above the water.

Therefore, this thesis investigates the design and creation of a water-propelled robotic system, keeping in mind the robot's primary function of traveling using water-jets through/on the water as well as in the air. Further, it investigates the expressibility of emotions and intentions of such a robotic design.

## 1.1 Prior Work

As discussed in the introduction, this thesis aims to create and develop a water-propulsion robot and use both the motions and water movements to express emotions. This section describes the current work regarding the creation of a water-propulsion system, quadcopter control, and emotion encoding.

In order to evaluate motions using water as a source of movement and expression, the water-propulsion system needed to be created and investigated. Therefore, to design the water-propulsion system, prior work was used to determine the details of generating thrust and lift using nozzle shape and pipe bends.

Then, with the creation of a system, the robot needs to be able to control the thrust to generate and execute motions. One of the most common robots capable of vertical or jumping motions are quadcopters. However, quadcopters are not able to traverse the same aquatic environments as the robot this thesis will focus on. But, if a designed aquatic robot can be structured similarly to a quadcopter, the control of the system for upward thrusts can be modeled in a similar fashion as well. Therefore, using four jets instead of four rotors, the robot aims to control and generate motion behaviors based on the control system of a quadcopter.

Finally, with the ability to encode robot motions and behaviors through jumping, tilting, and traveling, the final step is to use the motions to express emotions. In order to quantify emotions, the robot first needs a set of interaction characteristics to describe each motion and map that to an emotion. Then, using interaction attributes and a mapping to emotions, the robot can perform a sequence of motions to express emotions.

### 1.1.1 Water Propulsion

Since thrust is directly proportional to the mass flow rate, the pressure of a system, and water has a high density compared to air, using water as a rocket fuel for thrust increases the ratio between the force produced and volume expelled as described by preliminary calculations in [6]. Early work on water-propulsion involve applications such as waterjet cutting, the conversion of water pressure into kinetic energy, and flow through pipe bends [29, 30].

The thrust generated by water-propulsion is also directly linked to the shape and restriction of flow through the system. To minimize the loss of pressure, bend angles should be at a maximum of  $30^\circ$  angles with the most pressure loss being at  $90^\circ$  angles and greater [11, 30] with a radius lead for the shape of the exit nozzle [29]. Chapter 3 goes into more depth of the creation for various nozzle designs and their resulting thrust.

Most recently, water propulsion has been tested with less static structures tackling otherwise difficult problems, such as carrying heavy objects or producing single streams of greater force. Work has primarily focused on the development of water-propelled systems using humans to close the control loop of the system through direct remote control. A non-robotic water-powered jetpack focuses on using the water



Figure 1.1: Lin et al. [23] Spherical Underwater Water-Jet Robot (left) and Jetlev-Flyer (right)

to propel and stabilize a person in the air. Using a 30-pound jetpack, the Jetlev-Flyer can generate 430 pounds of thrust at 22 mph [3]. Lin et al. [22, 23] further extends the use of a water-powered system by creating a submersible spherical water-jet robot. Images of both water-propelled robots are shown on Figure 1.1.

### 1.1.2 Quadcopter Control

As Section 3.2 will later describe, the control system will be modeled after that of a quadcopter. However, unlike a quadcopter, the system will have negligible rolling moments, rotary actuators which typically cause significant control system complexity [12].

Quadcopter control can be modeled using basic dynamics, Denavit-Hartenberg, and Euler-Lagrange methods by looking at the desired roll, pitch, and yaw angles along with the resulting torques generated by each motor. Current work involving quadcopters are additionally typically simulated after generating equations of motion [16]. However, more recently, there has been further extensive work using PID, LQR, and LQR with Integral Backstepping to maintain online direct responses with zero attitude angles to stabilize the quadrotor from exterior disturbances such as yaw drift, sensor noise, and various other unmodeled effects [12, 15]. Furthering the concept of online predictions, approaches such as Nicol et al. [28] additionally delve into adaptive neural network control to perform stabilization.

Chapter 3 goes into further detail about controlling a water-jet system modeled after a quadcopter using PID control and its unique equations of motion. Additionally, the overarching system logic will be based on a typical quadcopter PID system.

### 1.1.3 Encoding Emotions

Quantifying and encoding emotions through robotic movements are becoming important problems as robots are found in more social situations. In particular, cooperation with direct verbal communication can help increase productivity and indicate problems to human operators. However, there are many different methods to determine how to quantify and create a robotic body language.

One of the most prevalent ways to encode emotions are through the use of the Laban characteristic scheme describing dance motions and the fluidity of expression in 3D space in [27, 34]. One of the main Laban characteristics focus on the Dynamosphere of eight basic efforts and their relationship to each other.

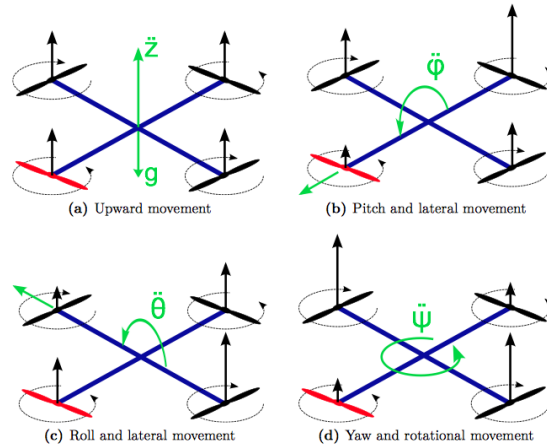


Figure 1.2: Quadcopter dynamics image detailing the different motions quadcopters can have and exert [31]

Knight and Simmons use the Laban characteristics and movement frequencies focusing on flow, space, time, and weight to describe robotic head-motions using the Keepon robot in and the expressive motions in X, Y, and Theta for mobile robots [19, 20]. Similarly Nakata et al. use Laban efforts to express emotion and intention through shapes of body movement and consciousness [26].

On the other hand, Lenz et al. create an Interaction Vocabulary identifying key interaction attributes and their extremes in [21]. And with the Interaction Vocabulary, Cauchard, et al. takes the encoding one step further encoding emotions in the movement patterns of drones [13] and mapping them to various personality profiles.

Like the Cauchard et al. paper, Chapter 4 looks at the encoding of emotions using the Interaction Vocabulary specifically regarding motion patterns using the described levels for interaction characteristics from [13].

## 1.2 Thesis Problem

This thesis covers the design decisions that were chosen to create an energy efficient water-propelled robotic system and control the robot, nicknamed *Firefly*. Then, using the created robot, this thesis investigates the expression of emotions through motion between *Firefly* and an aquatic environment. This task was accomplished by:

- Creating a unique water-propelled robotic system to enable regular and emotional motion.
- Using an existing emotion-encoding methodology to define behaviors of the robotic system.

## 1.3 Contribution and Outline

Chapter 2 delves into the mechanical and electrical design of our unique robotic system. The chapter begins with a discussion of the mechanical structure and design of the robot, including creating a water-resistant box to hold the electronics. This chapter also documents the electrical architecture and power constraints of the system. Chapter 3 describes the system using the concepts of water flow and jet propulsion and control systems. The chapter additionally compares and contrasts the propulsion nozzles and

their effectiveness against similar nozzle designs in various fluid flow papers. Chapter 4 describes how this novel robotic system is able to express emotions using the same water jets used for regular travel.



# Chapter 2

## Overall Design

### 2.1 Design of Mechanical Structure

Unlike quadcopters, our robot nicknamed *Firefly* is created with the ability to traverse on and above the water, and potentially in the future, below water. The unique structure of our robot and environment allows the motors and batteries to be sealed from potential leakage, removes the interference caused by rotor-generated wind currents, decreases the weight required on the robot, and increases the weight-thrust ratio for propulsion and lift.

*Firefly* has pumps, tubes, valves, and most of the electronic components off of the robot in a separate cart offboard tether which control the flow to *Firefly*'s jets. The robot only has sensory feedback components necessary for flight stored in a water-resistant plastic box onboard. To ensure water-resistance, the 3D-printed plastic resin box has a single opening for power input with a CAT-5 cable sealed with petroleum jelly.

Using a low-center of gravity disk modeled to create similar control behaviors as a quadcopter, *Firefly* is designed to be a robot propelled by four water jets. Water flows from the input stagnant pool water into two 100 psi pumps each of which supply two jets with water. The pump fills a water tank and then flows to each of the jets through 1/4" tubing and reaching the exit nozzle of 2mm. The resulting onboard system is shown in Figure 2.1 which travels on and above the water's surface.

By creating this mechanical system which can adjust the flow rate and thereby the strength and amount of splashes the water exhibits, *Firefly* is given both a form of movement and a way to manipulate water for use in the expression of emotions through motion.

#### 2.1.1 Overall Mechanical System Architecture

While the Lin et al. spherical underwater water-jet robot or water-powered jetpacks such as Flyboard and Jet-lev Flyer direct the jets toward opposite desired directions of travel, *Firefly* controls the rate of flow for each jet (much like a quadcopter to travel in a desired direction) [3, 23, 32]. Thus, the moving component of *Firefly* is able to reduce its weight significantly because it does not require an onboard gimbal or motor system to orient each jet's direction. A practical gimbal system for *Firefly* such as the one in Figure 2.2 would add well over 400g for each jet to the assembly.

Since the output force from each jet is a direct result from the restriction and amount of flow through the exit nozzles, restricting any flow before the nozzle output will reduce the amount of force produced. Thus, when water enters the system through a 1/2" entry point, the water moves to four nozzles through 1/4" tubing with no barb connections until the exit nozzle at 2mm.

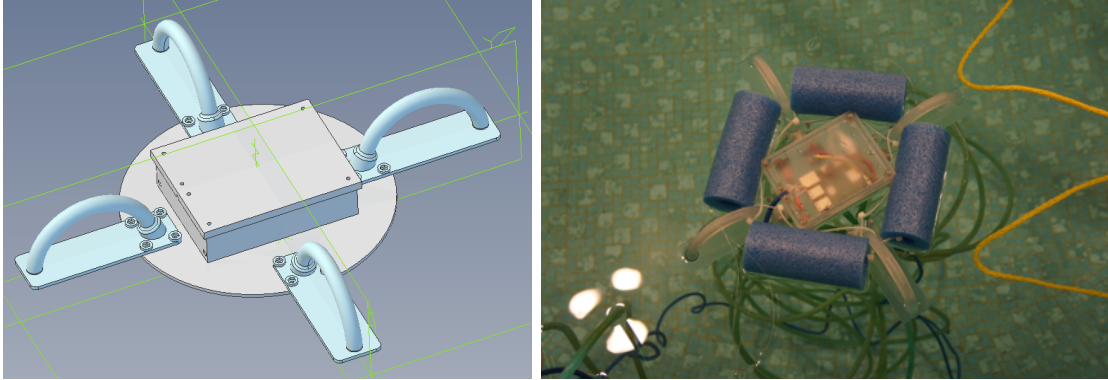


Figure 2.1: Created and Designed CAD model and prototype of *Firefly*.

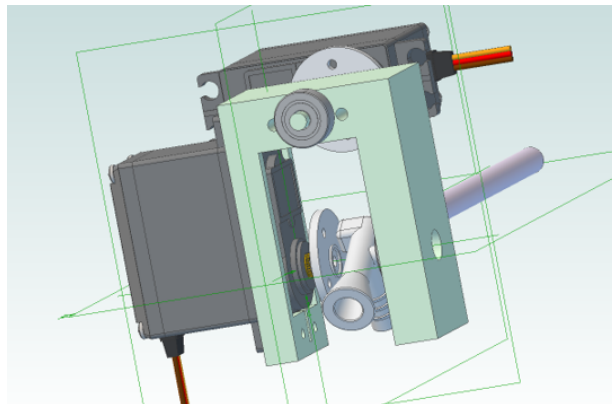


Figure 2.2: CAD drawing of a potential gimbal system to work onboard *Firefly* using waterproof servo motors with roughly 120oz-in of torque.

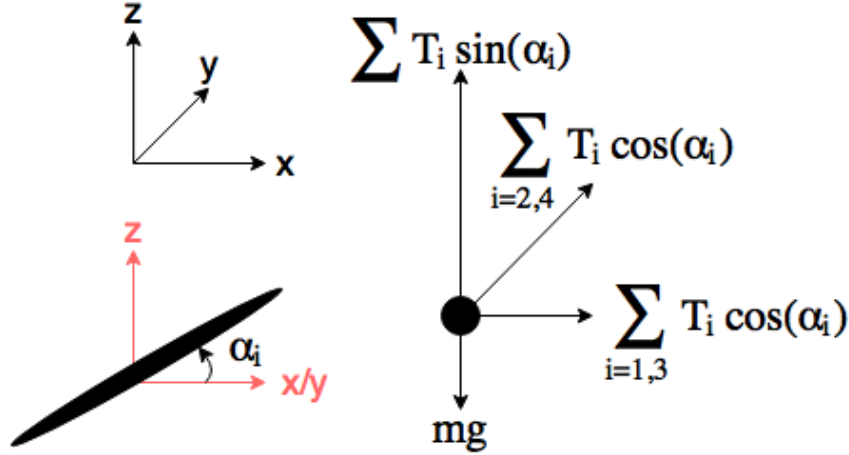


Figure 2.3: Free body diagram detailing the equations of motion for *Firefly*

Although the motor could be placed onboard and a valve opening varied to change the amount of thrust and force, each jet would add roughly 202.4g of weight on the *Firefly* per jet. In addition, one advantage of having the motors on board is the increased responsiveness and minimal delays for a response. However, since water pressure varies based on the speed of sound in water and there is roughly 25ft of tubing material, nozzle changes can be controlled at an estimated rate of 194Hz.

### 2.1.2 Low-Center of Gravity Disk

A rotationally symmetric, in the horizontal plane, robot was created with a nozzle on each of the four corners and a single electronic box in the center. All of the tubing runs from the pumps below *Firefly* and is brought up and attached to *Firefly* with push-connect connections. Since *Firefly* is 672.1g, symmetrically balanced, the majority of the mass is centrally located, and additional weight is caused by the water flowing through tubing below itself, the center of gravity for *Firefly* is centrally below the robot.

As will be discussed in Section 3.1.2, the thrust generated by each nozzle  $i$  at any given inlet water pressure can be determined as  $T_i$ . Thus, the equations of motion are as follows for each jet  $i$  and  $\alpha_i$  from horizontal:

$$F_{net,x/y} = \sum T_i \cos(\alpha_i) \quad (2.1)$$

$$F_{net,z} = -mg + \sum T_i \sin(\alpha_i) \quad (2.2)$$

Figure 2.3 also details the free body diagram of the system and the resulting net force acting on *Firefly*.

## 2.2 Design of the Electrical System

Designing the electrical system for robots can be challenging especially when dealing with chlorine or saltwater. The electronics can short circuit if they come into contact with the water and can present a fire or electrocution hazard if the robot draws power from a regular outlet. For these reasons, although *Firefly* is tethered to its control system away from water, the robot is powered from 12V and 14.5V batteries.

*Firefly* requires sensory inputs both from on-board and off-board of the propelled disk. All communication is sent via USB serial or through ethernet between on-board and off-board microcontrollers. By

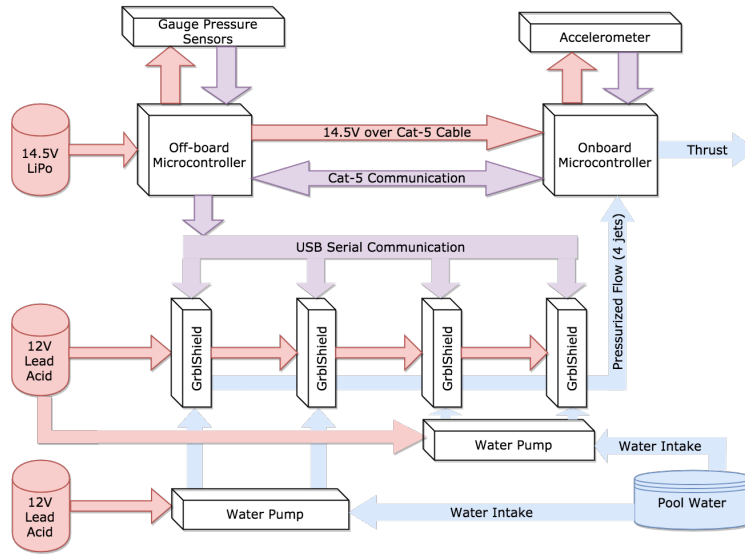


Figure 2.4: Electrical architecture diagram detailing the communication method and power distribution.

routing all communication through an off-board RaspberryPi, all data is processed in a single serial and synchronous control loop.

### 2.2.1 Overall Electrical System Architecture

On-board sensory data is communicated via a Raspberry Pi microcontroller to the motor and main control computations. The on-board microcontroller and all sensory boards and power converters are sealed within a single water-resistant box located in the center of the system. A single CAT-5 cable transfers power to the on-board microcontroller and communicates with an off-board Raspberry Pi microcontroller. The off-board microcontroller receives fluid pressure in the system for all 4 tubes and performs all computations regarding controls of the system.

Four Nema 23 stepper motors are used to control valve positions including shut-off. Each stepper motor is supplied 12V of power using a total of two lead-acid 12V batteries. Each stepper motor is linked through the Arduino grblShield open-source in [1] and then through USB serial to the main microcontroller. The microcontrollers are powered by a 14.5V LiPo battery and split via a CAT-5 cable to reach both the onboard and offboard systems. Figure 2.4 displays the overall electrical structure in further detail.

## 2.3 Discussion

*Firefly* can travel on and above the water, however, this particular design does require some input water source and must be tethered via water tubing. Using water-propulsion as the motion base also increases the weight-thrust efficiency for movements. In addition, the design of a low center-of-gravity can aid in stabilizing the system. And, since the water pressure can be obtained with a separately powered system from the part of *Firefly* performing motions, the amount of power required to sustain flight with separate and heavier batteries can also be subsidized rather than what can be carried on-board.

Due to the supply of power and the flow of water from a base station, *Firefly* also has its valves

and control motors on the base station. This lessens the amount of weight on-board that needs to be propelled. In addition, since the amount of wires can be limited by using tethered communication between the offboard and onboard microcontrollers, a single CAT-5 cable can supply power and communicate with *Firefly*. This method of having an offboard and onboard microcontroller also allows for the system to easily scale with additional onboard sensors such as cameras, altitude sensors, or GPS.



# Chapter 3

## Water-Propulsion System

### 3.1 Water Jet Nozzle Design

Water-propulsion is dictated primarily by the volume, pressure, and shape of the exit water flow. As discussed in Section 2.1.1, the flow of four jets were used over gimbals to control the robot due to the reduced weight and additional flow control to help with the expressibility of emotions. The overarching design was based on a quadcopter to create and generate similar vertical motions replacing the rotors with jets.

Thus, *Firefly* needs four single streams with the least loss in pressure, the exit nozzle is one of the most important parts of the system; any slight perturbations in the stream can cause a significant control change and can limit the maximum thrust the system can produce.

To maximize the amount of thrust that can be produced at a given flow and pressure, the fluid dynamics minor losses need to be minimized. According to Powell [29], the orifice or nozzle output geometry is a direct correlation to the coefficient of discharge, otherwise known as the reduction in output pressure. Additionally, there can be pressure losses due to a restriction in flow from curves or bends in the pipe. Depending on the turbulence and shape of the flow, pressure losses can be seen starting at any angle larger than  $30^\circ$  in the tubing to a maximum of any angle  $90^\circ$  and larger [11, 30]. Thus, *Firefly* attempts to minimize all bends and increase thrust through improvements in nozzle shape and designs.

#### 3.1.1 Nozzle Shape

Before the exit nozzle, the flow system for *Firefly* has an input of water flow with a cross-sectional area of  $1/4in$  and a pressure ranging from  $60psi - 100psi$ . As described in Section 3.1.2, the exit nozzle has an output diameter of  $2mm$ . Since our inlet opening is much larger than our orifice outlet and the stream needs to be as uniform and straight as possible [25, 29], the orifice should follow a radius lead shape to maximize theoretical efficiency for  $0.98 C_d$  over a straight edge of  $0.60 C_d$ . Figure 3.1 shows a flared inlet at the nozzle orifice to maximize flow and ultimately thrust.

The *coefficient of discharge*  $C_d$  of flow has the following defined relationship between the ratio of orifice edge radius  $r_{edge}$  to orifice bore diameter  $d$  from [29] as:

$$\Delta C_d(\%) = 5.5 * 10^3 \left( \frac{r_{edge}}{d} \right) \quad (3.1)$$

where  $C_d$  is the ratio of actual mass flow rate at the end of the nozzle to an ideal nozzle for water and the same exit pressures. Additionally, according to Szanislo [33] and Idris and Pullen [18], there is a direct positive correlation between the maximum coefficient of discharge at a ratio greater than or equal to two

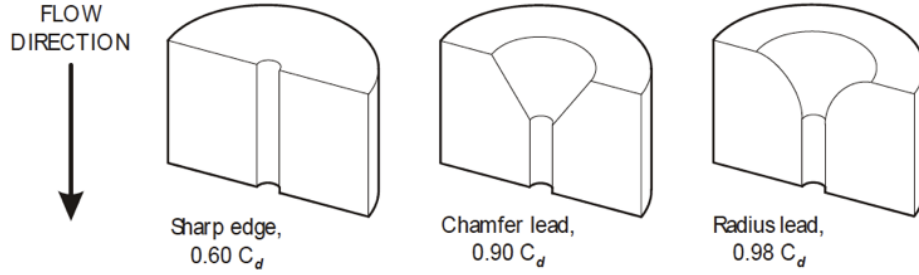


Figure 3.1: Taken from [29], nozzle exit orifices and the relationship to the coefficient of discharge  $C_d$  to maximize efficiency of flow.

for orifice radius and bore diameter. Thus, the designed nozzle was created with a ratio of two between orifice radius and bore diameter and a radius lead nozzle orifice.

Additionally, tubing bends can cause minor losses beginning at angles of  $30^\circ$  and increasing to a maximum at  $90^\circ$  and higher [11, 30]. Thus, for the *Firefly* exit nozzles, a ratio of exactly 2 : 1 between orifice radius lead edge and bore diameter was selected. Additionally, the total number of  $90^\circ$  and larger bends in the system were minimized. Thus, rather than using two  $90^\circ$  bends, the designed nozzle was created with a single radiused or semi-circular bend.

Thus, using the factors of nozzle shape and tubing bends, the following nozzle prototype design was created and shown in Figure 3.2.

### 3.1.2 Generated Thrust

Given the nozzle shape described in Section 3.1.1, the mass flow rate and generated force were empirically determined for various nozzle designs and overall mechanical structures changing the exit orifice area. However, determining thrust and mass flow rate of a water-propulsion system can prove to be quite challenging because the pressure of water cannot be measured with a direct stream.

One measurement system consisted of adding additional mechanical factors with a hinge and nozzle setup, where the thrust on one end of the hinge could be measured and water output could directly cause the force on the opposite end. However, inconsistencies with the system such as the lever and hinge weight and resistances can introduce additional variables into the system. A prototype testing jig for measuring thrust is shown on Figure 3.3.

The thrust and mass flow rate can be experimentally determined by calculating the change in mass over time. With reference to [5, 6, 7], the thrust  $T$  generated by the nozzle can be quantized as:

$$T = \dot{m}_e v_e - \dot{m}_0 v_0 + (p_e - p_0) A_e \quad (3.2)$$

where  $\dot{m}_e$  is the mass flow rate at the nozzle's exit,  $v_e$  is the velocity of water at the nozzle's exit,  $\dot{m}_0$  is the mass flow rate at the nozzle's inlet,  $v_0$  is the velocity of water at the nozzle's inlet,  $p_e$  is the atmospheric pressure,  $p_0$  is the water pressure at the nozzle's inlet, and  $A_e$  is the cross-sectional area of the nozzle's exit. Then, using the following formula created with reference to [2],

$$v = \frac{\dot{m}}{\rho A} \quad (3.3)$$

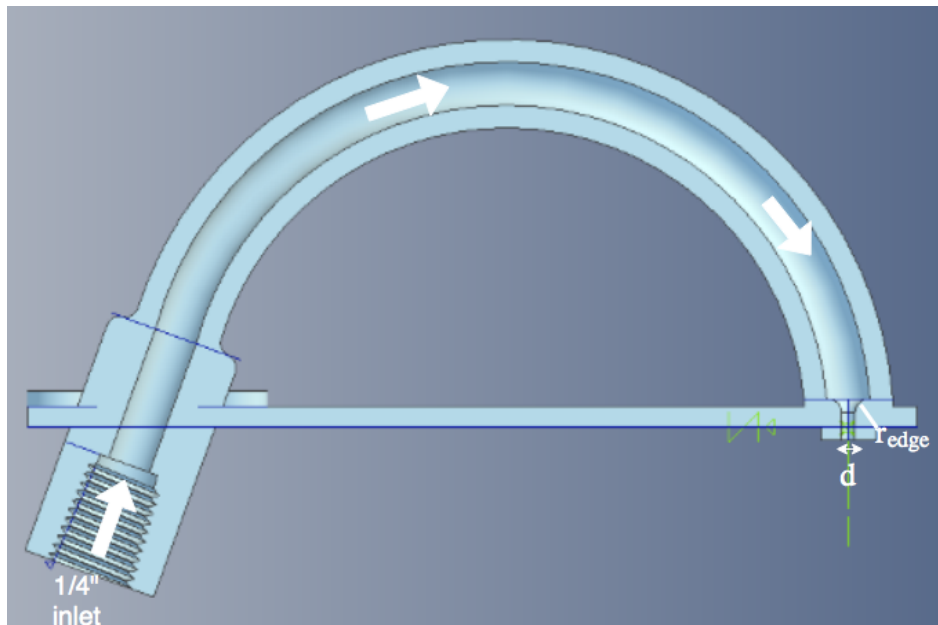


Figure 3.2: Prototype water-propulsion nozzle design for *Firefly*.

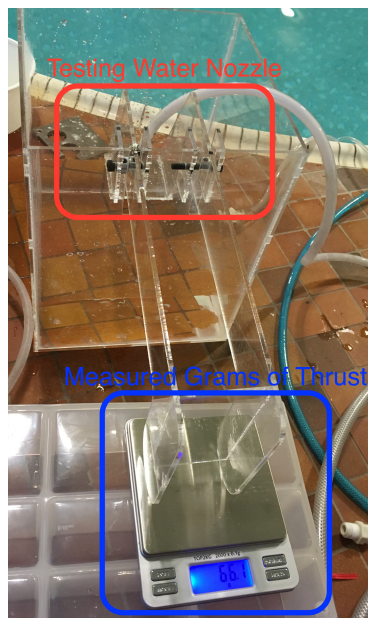


Figure 3.3: Thrust testing setup to measure the grams of force produced by a nozzle's propulsion. Nozzle is installed in the red box and measurements were read within the blue box. Nozzle force is converted into grams of thrust on the scale rotating on a single axle.

Table 3.1: Comparison between tube diameter with no nozzle (6.35mm), 1.5mm, and 2mm nozzles on average experimentally generated inlet pressure, elapsed time, mass flow rate, velocity, and thrust.

	Inlet Pressure [ $P$ ] ( $psi$ )	Time [ $t$ ] ( $ms$ )	Mass Flow Rate [ $\dot{m}$ ] ( $kg/s$ )	Velocity [ $v$ ] ( $m/s$ )	Thrust [ $T$ ] ( $N$ )
6.35mm	84.70	10055	0.15	4.64	15.97
1.5mm	76.63	10052	0.05	27.39	1.40
2mm	72.5	10093	0.08	24.55	1.92

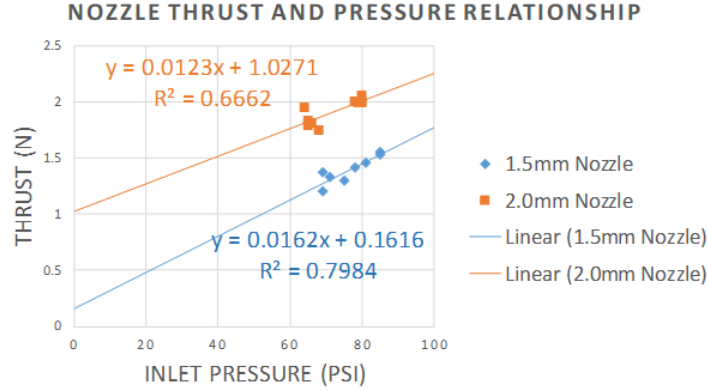


Figure 3.4: Experimentally determined relationship between thrust and inlet pressure on 1.5mm and 2.0mm nozzles with 8 – 10 measurements.

where  $v$  is any water velocity,  $\dot{m}$  is the mass flow rate,  $\rho$  is the fluid density, and  $A$  is the cross-sectional area of an orifice, the thrust is determined using only the nozzle exit area, mass over time, and inlet pressure.

Thus, the mass flow rate and inlet pressure would only need to be measured for thrust calculations. Additionally, the definition of mass flow rate  $\dot{m}$  with volume  $V$  and over time  $t$  can be determined as

$$\dot{m} = V/t \quad (3.4)$$

Table 3.1 shows the average pressure and change in expelled water for 1.5mm and 2mm nozzles at the maximum opening capacity with 8 to 10 measurements over a 10 second period. The mass flow rate, velocity, and thrust were calculated by applying equations (3.2), (3.3), and (3.4). Using the generated data for thrust, each jet is shown to have on average a maximum of 15.97N without a restriction on flow. However, the system is limited by the amount of output flow at a given pressure that must be maintained. Thus, the finalized nozzle was created to limit the amount of output flow while still producing thrust sufficient to support the robot’s weight. With the finalized 2mm nozzle, the thrust achieved was on average 2.10N, yielding a 33% increase in maximum thrust over the 1.5mm nozzles for inlet pressures around 75psi. Figure 3.4 extrapolates the data points to the maximum 100psi which the pumps in *Firefly* can output.

Additionally, the restriction of flow through valves causes increases in head loss. Therefore, lowering the valve opening, will decrease the generated thrust. To experimentally determine the relationship, one

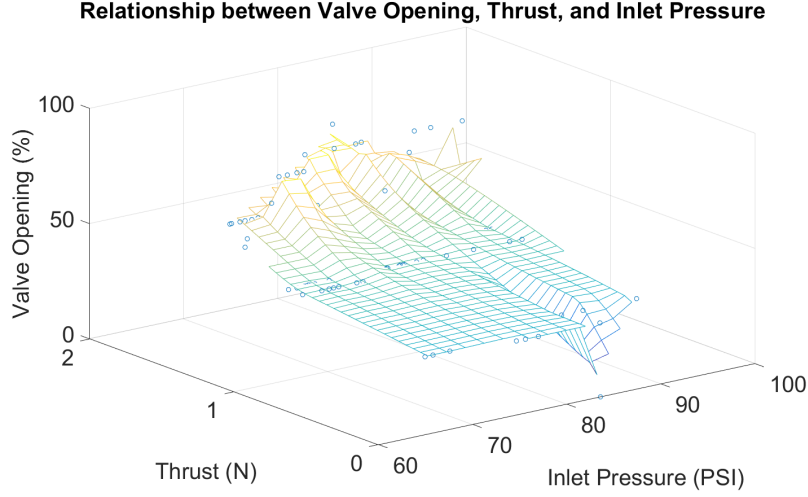


Figure 3.5: Experimentally determined relationship between thrust, valve opening, and inlet pressure on a 2.0mm nozzle with 102 measurements.

axis was restrained for *Firefly* and weights were placed on an opened jet, recording weight, pressure, and amount of valve opening. A table of values were generated when the accelerometer reading was nearly level, thereby detailing a balanced weight versus thrust ratio.

Figure 3.5 describes the relationship between valve, thrust, and pressure. Using external weights, *Firefly* was set off balance on the pitch axis. Then, when the thrust produced by the valve opening was sufficient to counteract the weight, the measurement was saved. The sufficiency criteria was determined as  $\pm 1^\circ$  angle of rotation from  $0^\circ$ . From Figure 3.5, it was determined that there was a negligible change of thrust based on pressure for small valve openings. Thus, pressure was factored into the PID control at different valve openings based on a linear relationship.

### 3.1.3 Efficiency Comparison of Nozzle Shape

As referenced in Section 3.1.1, the ideal coefficient of discharge  $C_d$  for a radiused lead nozzle is 0.98 compared to that of a straight edge of 0.60 [25, 29]. Since the coefficient of discharge measures the actual to ideal mass flow rate, the efficiency of a nozzle can be directly determined using  $C_d$  and the empirical mass flow rate.

Since pressure for *Firefly* ranges from 60psi – 100psi and operates with water at a temperature of 77°F, referencing [9], the following formulas for coefficient of discharge  $C_d$  for water are shown as:

$$C_d = \frac{Q_w}{0.07785 \cdot \left(\frac{d_0}{4.654}\right)^2 \cdot K_c} \quad (3.5)$$

with  $Q_w$  as the water flow rate,  $d_0$  as the orifice diameter, and where  $K_c$  is represented with the following formula for the measured pool water of 77°F:

$$K_c = \begin{cases} \sqrt{\frac{p_1 - p_2}{SG}} & p_1 - p_2 < 0.9^2 \cdot (p_1 - FF \cdot 23.8) \\ \sqrt{\frac{p_1 - FF \cdot 23.8}{SG}} & p_1 - p_2 \geq 0.9^2 \cdot (p_1 - FF \cdot 23.8) \end{cases} \quad (3.6)$$

Table 3.2: Comparison using the coefficient of discharge between the constructed and ideal nozzle shape for both straight edge and radius lead orifices.

	Straight Edge Orifice	Radius Lead Orifice
$C_d$ Efficiency	1.21	0.74
% $C_d$ Error	-20.8	+26.0

for inlet pressure  $p_1$  between  $60psi - 100psi$ , outlet pressure  $p_2$  at room temperature, and the critical pressure ratio factor for water  $FF$  determined by [4] and defined as:

$$FF = 0.96 - 0.28 \sqrt{\frac{p_1}{225.56 \frac{kg}{cm^3}}} \quad (3.7)$$

Using the mass flow rate empirically determined and then extrapolated in Figure 3.4, the thrust  $T$  of *Firefly* for  $2mm$  nozzles and inlet water pressure  $P$  is:

$$T = 0.0123P + 1.2062 \quad (3.8)$$

yielding  $\dot{m} = 0.0812 kg/s$  for  $100psi$  inversely determined by additionally using equation 3.2. Thus, the  $Q_w$  of the system is  $0.292 m^3/h$ . Using equation 3.5,  $C_d = 0.725$ . Since, in an ideal case, nozzle with orifices of straight edge have  $0.6C_d$  and radius lead have  $0.98C_d$  the efficiency of nozzle shape can be shown in Table 3.2.

## 3.2 Software System Architecture

Due to the unique mechanical and electrical architecture of *Firefly*, the system requires multiple different sensory inputs and motor control schemes. The software is synchronously run with a single serial control loop dictating the state flow of the system. Thus, the main control must communicate through interprocess communication to the onboard sensors and USB serial to the motors as detailed in Figure 3.6.

When performing interprocess communication, each background process is run simultaneously and responds to queries sent by the main executing control loop. All responses are blocking calls and are kept to a maximum of 3 milliseconds - this allows for a tight control loop with higher responsiveness to sensory changes. Not only does the separate processes offload computation, but it also allows response status from sensors to be monitored and an additional motor communication queue (required by the internal software of the GrblShield).

### 3.2.1 Control Algorithms

Similar to quadcopters, a PID controller with active error correction was implemented on the *Firefly* [15]. While quadcopters need to adjust the thrust taking into account the rotary moments created by the spinning propellers, a water-propelled system such as *Firefly* does not have those limitations. In addition, multiple PIDs also take into account error feedback from wind currents or changes in air pressure. Due to the unique construction, variances in air do not impact the robot as heavily and are not required to be taken into account.

The control system consists of two PID loops that are used for maintaining a desired roll and pitch. Altitude is maintained by controlling the total sum of jet openings. Each PID loop adjusts the jet openings

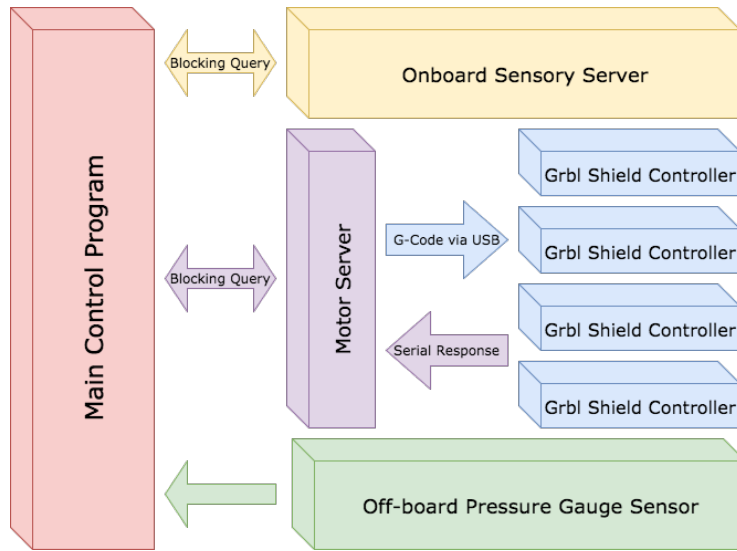


Figure 3.6: Software system architecture block diagram detailing the communication scheme between sensors, motors, and the main control loop and system state

(Figure 3.7). Two of the four jets control either roll or pitch and are physically chained together to the same of the two pumps so that small variances in flow and pressure can be mitigated. The control system then adjusts the jet openings of the associated roll or pitch accordingly. Although the robot can balance both roll and pitch well, *Firefly* is unable to sustain flight without drifting uncontrollably due to unpredicted forces from the hose and drag of the hose underwater.

Thus, while *Firefly* uses a PID to control behaviors and increase stabilization, neural networks were also investigated as a possible way to improve jet positioning based on sensory saved data from the PID algorithm, like the systems shown in [28] with a structure of Figure 3.8.

However, due to the lack of labeled data and variances in performances based on desired movement, the neural network did not perform well enough to be used, yielding a 18% accuracy rate.

### 3.3 Discussion

The water nozzle design achieved a 20.8% improvement in the coefficient of discharge over a straight edge showing a significant boost due to our design implementation in the resulting thrust with an empirically determined relationship with pressure (3.8). Additionally, the impact of thrust was compared with a 0.5mm increase in the nozzle bore orifice (Figure 3.4).

Due to the complexity of the system and unique mechanical and electrical design, the software system architecture consisted of multiple interprocess communication as well as status monitoring. As detailed in Figure 3.6, the open-sourced GrblShield must additionally transmit periodic status notifications and a process is required to wait on them. Then, using a PID control system structured to control four jets (Figure 3.7), minimal stability and orientation was achieved. However, the unpredictable forces from both the water and drag of the hose proved to negatively impact the PID and full flight stability was not achieved. A neural network alternative was not able to reach an acceptable level of performance, given the data available at the time.

However, the PID control of the system did allow for valve position control and thus to a desired tilt and thrust for the *Firefly*. Using the sensory inputs of two pressure gauge sensors and an accelerometer, the

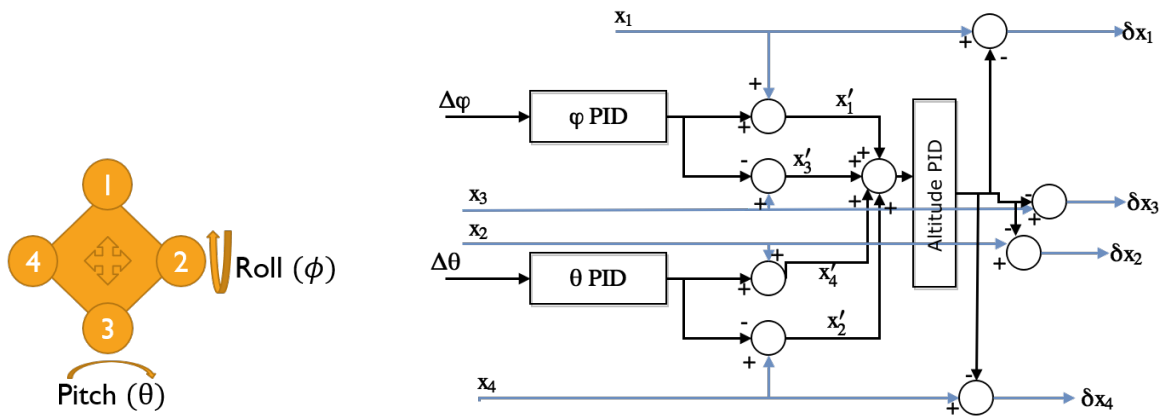


Figure 3.7: There are three major PID loops which control the stability and altitude of the robot. The jet  $i$  position  $x_i$  is adjusted with each corresponding PID, ultimately resulting in  $\delta x_i$  for the final adjusted jet position which is then commanded to the motors.

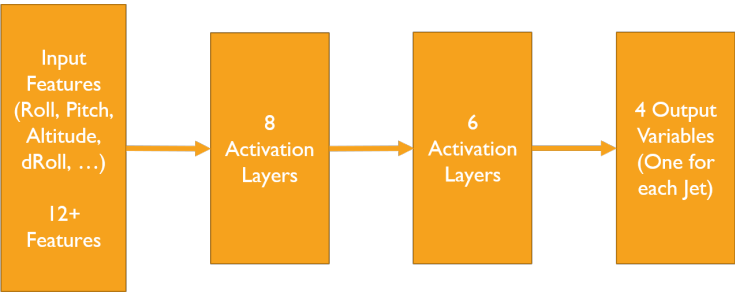


Figure 3.8: The neural network architecture was used to better approximate the correlation between a sensory input space of over 12 features to the best predicted jet nozzle opening for each of the four jets. Activation layers of sizes 8 and 6 were used as the internal components of the neural network.

system was able to use a PID to output desired roll, pitch, and altitude (or total thrust) for *Firefly* through the adjustment of valve openings. These valve openings allowed the system to vary the total amount of output flow each of the nozzles produced, and thus, the total thrust from each jet of *Firefly*. Thus, *Firefly* was able to create controlled movements specified by tilts and thrust percentages.



## Chapter 4

# Expression of Emotions from Motion Profiles

The expression of emotions is becoming an important challenge in the robotics industry as robots and humans are increasingly found in more interactive situations. Using the Interaction Vocabulary of Lenz et al. [21], the motions and patterns of robotic movement can be quantified into readable terms and then executed accordingly. Similar to the methods of encoding emotions in drones by Cauchard et al. [13], *Firefly* quantifies and performs a series of motions to express emotions.

The investigation of emotions through motion is not only limited to robotics, but it also gains interests for stage variances and unique mediums. Most recently, FlyBoards have begun appearing in shows centered around the idea of water sprays, one image of which is shown in Figure 4.1 [8]. Rather than the movements created by a robot or person being the primary way to evoke an emotion, the water spray, splashes, and bubbles also change the message portrayed. Since *Firefly* is operated in a pool of water like the FlyBoard, this thesis hopes to investigate the production of emotions through movement as well as the interaction with objects and the environment.



Figure 4.1: Water effects using FlyBoard as part of a water show [8].

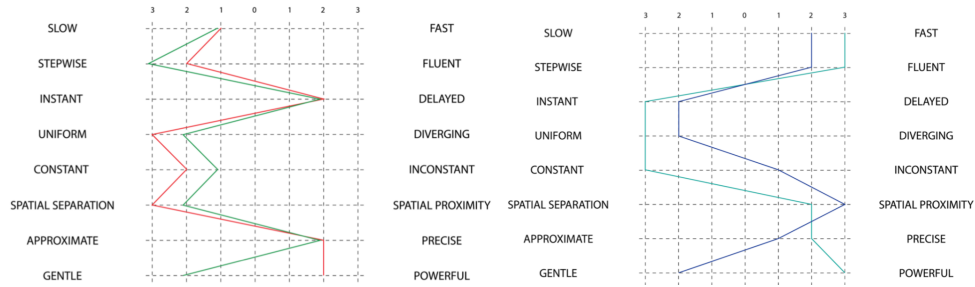


Figure 4.2: Taken from [13], interaction profiles are detailed using Interaction Vocabulary [21]. On the left, the encoding for grumpy (red) and shy (green) profiles are shown. On the right, the encoding for happy (blue) and brave (green) are shown. These drone-interaction profiles were developed by Cauchard et al. through a 5-person study assigning stereotypes of personality to Interaction Vocabulary characteristics.

Table 4.1: Description of Interaction Vocabulary created with reference to [21] regarding *Firefly* and its movement patterns.

Interaction Attributes	Description
Speed	How fast to perform the movement pattern
Fluency	How connected the current motion is to the next
Delay	How fast the robot reacts to interaction or environment changes
Divergence	How realistic and constant the movement patterns change
Consistency	Same action, same effect
Separation	Distance from the interaction object or person
Precision	Returning to the same movement location
Power	How bold or dangerous versus how elegant

## 4.1 Creation of Motion Profiles

Cauchard et al. [13] describes a method of mapping each emotion to the Interaction Vocabulary described by [21]. Using the profiles shown in Figure 4.2, each motion is mapped with similar attributes on the spectrum, where the range for each characteristic represents the minimum and maximum values possible of the *Firefly* system. Each listed attribute can be quantified and interpreted by the system (Table 4.1) created with reference to [21].

Using each motion created by the profile, a sequence of motions, such as jumps forward or tilt angles, were formed. Pairing various jumps and tilt angles, the movements were then put together with an interaction object to portray the desired emotion. Although the emotional model space for *Firefly* is different than that of drones described in [13], the overall mechanical design is similar and based on quadcopters. Thus, the breakdown of emotions into Dopey/Sleepy/Sad, Grumpy/Shy, Happy/Brave created from Cauchard et al’s [13] workshop study can be extended.

Two particular movements that were attempted for the portrayal of emotions were happy and shy behavior patterns. The happy or shy movement is created with a series of jumps and motions where the time delay, power, duration, etc. were varied according to the maximum and minimum behavior of the system shown in Figure 4.2.

Some of the major factors in the Interaction Vocabulary which differ between the happy and shy profiles are the separation and fluency attributes (Table 4.1, Figure 4.2). Thus, *Firefly* capitalizes on both the distance from an interaction object and the pauses between movements to help distinguish shy and happy behaviors. As Section 4.2 will describe, happy motions typically keep a close proximity and perform actions more rapidly with the interaction object while shy motions are the opposite.

Since the jets act as separate oppositely-paired thrusters, it is possible to do more expressive motions such as flips, jumps, and tilts. However, if the jets of *Firefly* were on gimbals, additional expressive behaviors such as rotation in place would be possible. These behaviors, while additive to the overall expressive movement, would likely not alter the portrayal of emotions than those of *Firefly*. However, a further study is necessary to determine the level of expression that spinning in place can give.

Additionally, using the paired thrusters allows an easy way to tilt in a desired movement direction and thereby show motion intentions. This deliberate tilt-and-move gives non-verbal cues to a bystander that the robot is intentionally moving toward or away from an object. Since the speed of travel is also heavily dependent on the angle of tilt, in addition to the amount of thrust, the robot will have a more drastic tilt if it wants to travel more rapidly. This can also prove detrimental and limit the amount of expressibility since the water spray is clearly visible in the system. However, in the resulting behaviors that were focused on, the system is supplemented through the expression of disliking or disregarding an interaction object - it seemingly turns sharply away and travels quickly while shooting the object backward.

With this clear concept and distinction, as described by Cauchard et al. [13], the expression of emotions is extended from drones to a water-propulsion robot structured similar to *Firefly* by creating profiles which match the appropriate range for each attribute and matching them with tilt angles and thrust.

## 4.2 Resulting Motion Behaviors

### 4.2.1 Happy Behavior

The key characteristics of happy behavior involved jumping and keeping a close proximity with the desired interaction object. Figure 4.3 shows the resultant behavior when *Firefly* performs interactions with rubber ducks. Physical contact with the ducks can also add to the creation and performance a playful happiness emotion. Each jump and movement is shortened to the specifications as discussed in Section 4.1 detailed by Cauchard et al. in [13]. Additionally, splashes in the water can add to the atmospheric effect, unlike emotion investigations in other mediums. Each length and depth of a splash as well as the distance of each splash can give depth to the robot's expressiveness unlike that of a quadrotor in air or similar medium.

As such, the movement of *Firefly* in Figure 4.3 details motions which stay in close proximity to the interaction object (rubber ducks in the video). *Firefly* first quickly approaches, navigates around, and then hops toward the ducks. This motion pattern is repeated several times, each ending with the robot in a closer position to the interaction target than the last. And, by keeping the closer proximity, *Firefly* might be shown not to have a perceived fear of the object which aids to the expression of happiness.

### 4.2.2 Shy Behavior

Compared to the happy behavior, the key characteristics of shy behavior involved fast jumps away from the desired object and consistently keeping distance from the desired interaction object. Figure 4.4 shows the resultant behavior when *Firefly* performs interactions with rubber ducks. Physical contact with the ducks must not occur to the insecurity of the robot for a shy emotion. Each jump and movement is lengthened per specifications as discussed in Section 4.1 detailed by Cauchard et al. in [13].

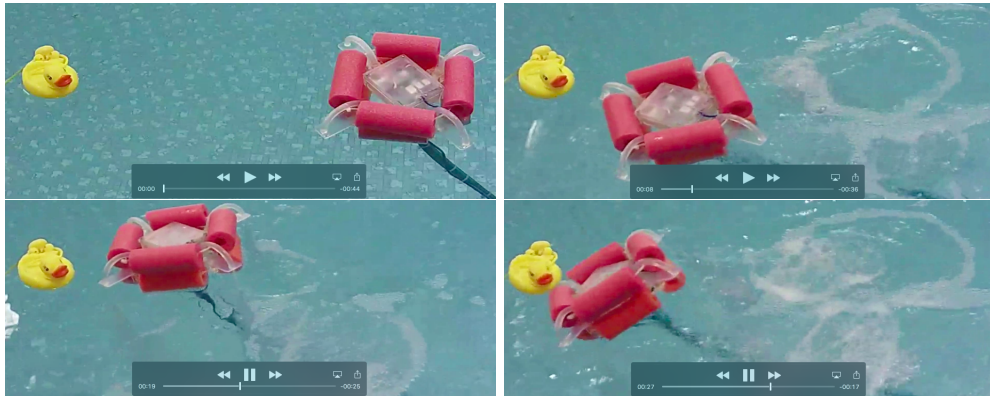


Figure 4.3: Storyboard of happy behavior movement through time steps. *Firefly* rapidly hops toward and approaches the interaction object (rubber ducks) from multiple angles. The robot always stays within close proximity of the ducks and occasionally bumps the ducks.



Figure 4.4: Storyboard of shy behavior movement through time steps. *Firefly* slowly approaches the interaction object (rubber ducks) from multiple angles. The robot always keeps distance between the ducks and never physically bumps the ducks. Additionally, *Firefly* will rapidly hops or moves away from the ducks after some amount of time approaching them.

Figure 4.4 minimizes large splashes toward the object allowing for a duration between interactions and denoting a lack of excitement when approaching the object as well creating a depth only strictly limited to the aquatic environment. Approaching slowly to the interaction target (ducks), the robot cautiously navigates its approach and then rapidly moves away from the target. The distance that *Firefly* moves away, after the approach, with the shy movement is significantly larger than that of the happy behavior. Additionally, the ducks are never interacted with, but *Firefly* approaches them very closely. These unique differences and using the concept of stationary ducks allow the user to perceive a sense of cautiousness while interacting with the same object.

### 4.3 Discussion

Using the emotion encodings for drones discussed by [13] and the Interaction Vocabulary in Table 4.1 created with reference to [21], *Firefly* was able to create new behavior patterns to match similar emotions.

There is a perceivable difference between movements created for the happy versus shy emotions that both expresses intent for movement without changing the method of travel. As described in Section 4.1, the level of tilt with oppositely-paired thrusters and the level of thrust achieved will both allow the robot to express intent as well as determine the level of power and direction of travel. This form of movement can thus express both the body language of travel and produce the desired motions and effects.

In particular, the happy motions both keep close proximity to the interaction object (rubber ducks) and create a perception of interest by limiting the tilt angle and amount of thrust. Since the distance and speed of travel is directly proportional to the tilt angle, a smaller tilt angle will allow *Firefly* to maintain close quarters with the object as well as subtly indicate to bystanders the intended direction of travel. Whereas, in the shy behavior, *Firefly* uses large tilt angles to both jump away quickly as well as indicate timid behaviors after approaching the interaction object.

While a formal study was not performed on the resulting motion behaviors, there is a clear distinction between the happy and shy movement patterns. Happy behaviors have a bounding and quick approach to the object, while, shy behaviors have a slow and cautious approach. These kinds of key differences in interaction attributes can characterize the scene and portray unique emotions. In addition, adding the fluency of water, splashes, and bubbles, can really aid to a performance of the robot. Each motion is accented and then visualized by the rippling effects and motions imparted on the water. As Section 4.1 described, when *Firefly* tilts and moves in a direction, the jets create bubbles and splashes in the opposing direction. In this way, you can visually see both the robot's speed and direction of travel through the effects of water in every frame.

So, using the interaction attributes, *Firefly* was able to roughly portray both the happy and shy emotions through movements and aquatic interactions.



# Chapter 5

## Conclusion

### 5.1 Summary

Water-propulsion can provide a new form of locomotion and open new horizons in both the utility and expressiveness of robotics. In fact, little is known about how to generate behaviors for the scale of this robot and how to more efficiently utilize water as both a propellant and method of interaction.

The unique water-propelled four-jet robot described here, nicknamed *Firefly*, uses simple equations of motion and a controllable movement pattern. The control of the system is based off of a quadcopter to produce the vertical motions for a desired roll, pitch, and altitude. At each of the four corners of the robot, thrust is produced by water-jet nozzles to propel the robot in a desired direction. The total forces are then controlled by the water flow rate out of the water jets and is restricted by pressurized flow through stepper-controlled brass valves. Although *Firefly* is built for locomotion above or on the surface of water, the same concepts can be applied to the system below water. As shown by the underwater water jet spherical robot created by Lin et al. in [22, 23], pressurized water is shot through water jet openings to propel the spherical robot in the opposing direction. Due to the construction of *Firefly* with off-board motors and only a single water-proofed electrical sensor box, it is also possible to create a system to travel underwater by removing the flotation devices.

One of the less prominent, yet crucial, investigations is on the behavioral spectrum. With the expression of emotions and intent, we can portray unique and distinct messages to viewers and coworkers without explicit communication, potentially saving time and promoting safety in a workplace [26]. Reflecting on the emotional model space for drones created by Cauchard et al. [13], *Firefly* attempted to express emotions through the aquatic environment and its motion patterns.

Using the quantified Interaction Vocabulary from Lenzet al. [21], *Firefly* expresses emotions by scaling the total possible range by limits of the motion patterns, dividing it equally, then choosing the portion of range dictated by Cauchard et al. for a desired emotion. The two most prominent emotions selected were the happy/brave and the grumpy/shy profiles. By using the descriptions of Interaction Vocabulary, each motion was created to match the attribute with environmental interactions and then placed in sequence to create a full interaction story. Although a full study on the behavior and motion patterns of the system was unable to be completed, Section 4.2 shows promise in evoking emotions from movements in and using an aquatic environment.

Through the creation of a unique water-propelled robot, the interaction created by the aquatic space was investigated. Focusing on the development and optimization of water-propulsion and the creation of behaviors to evoke emotions, this thesis hopes to have tackled the construction and details of robots with similar operating environments and constraints.

## 5.2 Limitations

Due to time constraints, there were several limitations which could be improved in future work: PID control, flight stability, a formal study on emotion behaviors, and emotional movements in 3D space above the water. Additionally, the system is limited based on hose length connected to an off-board system.

Although a PID control model was created for the system and was able to achieve stability when constrained for short periods of time, it is important to note that over time the control became increasingly unstable. We believe two reasons for the uncontrollability were forces from the hose inflexibility and drag under the water. The hoses induce moments on the actual device significantly and counteracting those spring-like and drag forces requires much more thrust than that which we could output. Section 5.3 discusses a possible way to create a future version of *Firefly* that should have negligible forces from a more flexible hose.

Another reason for instability may have been due to delays in the control loop. Although operations could be performed at a rate of  $194Hz$ , it might be possible that a PID system would be unable to generate responses fast enough to compensate for the delay in generated thrust from flow control on an offboard system to the nozzle output. Likely, a more complex control system would aid significantly in stabilization.

Further, this system created emotional behaviors which attempted to look visually appealing and evoke particular emotions. To accurately and systematically evaluate the behaviors, each should be run through a proper study to determine the boundaries on behaviors of the system. Thus, it is important to note that there is no quantifiable measurements on the behaviors.

Additionally, although the system has the ability for flight and the ability for underwater behaviors, motions and traversability in 3D space under and above the water were not heavily investigated. While it is believed that the system would be able to interact and move in both mediums, this thesis does not examine performance in these operating environments.

Lastly, the use of off-board power is both a benefit and a limitation. While there are many benefits to an off-board system such as power supplies, a contained system would allow traversal into less restricted environments. In order to accomplish this, it would be required to have both a powerful and light pump and an input source of water, whether from the surrounding area if in a body of water or from a water hose. The system would additionally need to be of larger scale with a greater amount of exit flow.

## 5.3 Future Work

As discussed in Section 5.2, the pull and drag of the semi-flexible hose caused significant forces on the system and thereby instability with movements. Primarily, it is thought the cause is due to the high forces raised by the tubing and the low thrust created by the system. However, with a more flexible tubing and a larger mass with more thrust, the induced forces will become negligible as the system's mass would be much harder to manipulate by drag and stiffness. Thus, future work could also continue the investigation of scaling the robot's size and propulsion forces to generate a much more stabilized system.

Additionally, the robot, *Firefly*, opens the possibilities of new methods of flight, broadening the horizons for potential applications such as fire-fighting or boat inspection. A possible extension of this robot could include the best of a submarine, boat, and quadcopter through traversal of all three different environments involving water: below, on, and above water locomotion. In addition to traversal through all three mediums, each environment can spur on a unique emotional behavior space for the robot which can be further investigated and studied.

Each new environment can heavily impact the behaviors and perception of motions and, thus, the personifications of a robot. When *Firefly* creates water effects in or above the water, a jet stream can

be visibly seen and can add factors to the overall show or portrayal of behaviors. However, moving to environments, such as below the water or movements through all three aquatic mediums, can add various complexities and an effective degree of freedom to the personification of the robot as a whole. The idea of creating and imparting changes to the environment through motion opens immense possibilities to the realm of portraying emotion in robotics. Thus, a further study could investigate the degree that motion generated environmental changes can impart the perception of robot intent.



# Bibliography

- [1] grblshield. URL <https://www.synthetos.com/project/grblshield/>. 2.2.1
- [2] URL [http://web.mit.edu/16.unified/www/FALL/systems/Lab\\_Notes/wrocket.pdf](http://web.mit.edu/16.unified/www/FALL/systems/Lab_Notes/wrocket.pdf). 3.1.2
- [3] A water-powered jetpack, Jul 2009. URL <https://www.popsoci.com/diy/article/2009-07/water-powered-jetpack>. 1, 1.1.1, 2.1.1
- [4] Flow rate calculation method of valve, 2011. URL [http://www.samshinvalve.co.kr/m/pdf/t\\_02.pdf](http://www.samshinvalve.co.kr/m/pdf/t_02.pdf). 3.1.3
- [5] General thrust equation, Jun 2014. URL <https://spaceflight systems.grc.nasa.gov/education/rocket/thrsteq.html>. 3.1.2
- [6] Rocket thrust summary, May 2015. URL <https://www.grc.nasa.gov/www/k-12/airplane/rktthsum.html>. 1.1.1, 3.1.2
- [7] Rocket thrust equation, May 2015. URL <https://www.grc.nasa.gov/www/k-12/airplane/rockth.html>. 3.1.2
- [8] Flyboard-show website, 2017. URL <https://www.flyboard-show.com/>. (document), 4, 4.1
- [9] Calculator: Water flow rate through an orifice, 2017. URL <http://www.tlv.com/global/II/calculator/water-flow-rate-through-orifice.html?advanced=on>. 3.1.3
- [10] Evan Ackerman. Why you want your drone to have emotions, Mar 2016. URL <https://spectrum.ieee.org/automaton/robotics/drones/why-you-want-your-drone-to-have-emotions>. 1
- [11] Karl Hilding Beij. *Pressure Losses for Fluid Flow in 90 [degree] Pipe Bends*. National Bureau of Standards, 1938. 1.1.1, 3.1, 3.1.1
- [12] Samir Bouabdallah and Roland Siegwart. Full control of a quadrotor. In *Intelligent robots and systems, 2007. IROS 2007. IEEE/RSJ international conference on*, pages 153–158. Ieee, 2007. 1.1.2
- [13] Jessica Rebecca Cauchard, Kevin Y Zhai, Marco Spadafora, and James A Landay. Emotion encoding in human-drone interaction. In *The Eleventh ACM/IEEE International Conference on Human Robot Interaction*, pages 263–270. IEEE Press, 2016. (document), 1.1.3, 4, 4.2, 4.1, 4.1, 4.2.1, 4.2.2, 4.3, 5.1
- [14] Eric Cheng. Drowned drones: When a multicopter hits the water. *Make*, Jan 2014. URL <https://makezine.com/2014/01/22/drowned-drones-when-a-multicopter-hits-the-water/>.
- [15] DM Filatov and AV Devyatkin. Quadrotor control system. 1.1.2, 3.2.1

- [16] Daniel Gheorghiuță, Ionuț Vîntu, Letiția Mirea, and Cătălin Brăescu. Quadcopter control system. In *System Theory, Control and Computing (ICSTCC), 2015 19th International Conference on*, pages 421–426. IEEE, 2015. 1.1.2
- [17] Guy Hoffman and Wendy Ju. Designing robots with movement in mind. *Journal of Human-Robot Interaction*, 3(1):89–122, 2014. 1
- [18] A Idris and K Pullen. The influence of chamfering and corner radiusing on the discharge coefficient of rotating axial orifices. In *IOP Conference Series: Earth and Environmental Science*, volume 16, page 012110. IOP Publishing, 2013. 3.1.1
- [19] Heather Knight and Reid Simmons. Expressive motion with x, y and theta: Laban effort features for mobile robots. In *Robot and Human Interactive Communication, 2014 RO-MAN: The 23rd IEEE International Symposium on*, pages 267–273. IEEE, 2014. 1.1.3
- [20] Heather Knight and Reid Simmons. Laban head-motions convey robot state: A call for robot body language. In *Robotics and Automation (ICRA), 2016 IEEE International Conference on*, pages 2881–2888. IEEE, 2016. 1.1.3
- [21] Eva Lenz, Sarah Diefenbach, and Marc Hassenzahl. Exploring relationships between interaction attributes and experience. In *Proceedings of the 6th International Conference on Designing Pleasurable Products and Interfaces*, pages 126–135. ACM, 2013. (document), 1.1.3, 4, 4.2, 4.1, 4.1, 4.3, 5.1
- [22] Xichuan Lin and Shuxiang Guo. Development of a spherical underwater robot equipped with multiple vectored water-jet-based thrusters. *Journal of Intelligent & Robotic Systems*, 67(3):307–321, 2012. 1, 1.1.1, 5.1
- [23] Xichuan Lin, Shuxiang Guo, Koujirou Tanaka, and Seji Hata. Development of a spherical underwater robot. In *Complex Medical Engineering (CME), 2011 IEEE/ICME International Conference on*, pages 662–665. IEEE, 2011. (document), 1, 1.1, 1.1.1, 2.1.1, 5.1
- [24] Robert Mahony and Vijay Kumar. Aerial robotics and the quadrotor. *IEEE Robotics and Automation Magazine*, 19(3):19, 2012.
- [25] McNally. Approximate flow through an orifice. URL <http://www.mcnallyinstitute.com/13-html/13-12.htm>. 3.1.1, 3.1.3
- [26] Toru Nakata, Tomomasa Sato, Taketoshi Mori, and Hiroshi Mizoguchi. Expression of emotion and intention by robot body movement. In *Proceedings of the 5th international conference on autonomous systems*, 1998. 1, 1.1.3, 5.1
- [27] Jean Newlove and John Dalby. *Laban for all*. Taylor & Francis US, 2004. 1.1.3
- [28] C Nicol, CJB Macnab, and A Ramirez-Serrano. Robust neural network control of a quadrotor helicopter. In *Electrical and Computer Engineering, 2008. CCECE 2008. Canadian Conference on*, pages 001233–001238. IEEE, 2008. 1.1.2, 3.2.1
- [29] Mark Powell et al. Optimization of uhp waterjet cutting head, the orifice. *Flow International, while the date of the publication is unknown, it is believed to be prior to Aug*, 19:19, 2009. (document), 1.1.1, 3.1, 3.1.1, 3.1.1, 3.1, 3.1.3
- [30] M. Rowe. Measurements and computations of flow in pipe bends. *Journal of Fluid Mechanics*, 43(4):771–783, 1970. 1.1.1, 3.1, 3.1.1
- [31] Saleh Said. Uav society, Jan 1970. URL <http://uav-society.blogspot.ca/2014/06/quadcopter-mechanics.html>. (document), 1.2

- [32] Sam Sheffer. The future of water sports is flyboarding, hoverboarding, and ver-ruckt, Jun 2015. URL <https://www.theverge.com/2015/6/26/8850777/hoverboard-water-flyboard-worlds-tallest-waterslide-top-shelf>. 2.1.1
- [33] Andrew J Szaniszlo. Experimental and analytical sonic nozzle discharge coefficients for reynolds numbers up to  $8 \times 10$  to the 6th power. 1975. 3.1.1
- [34] Rudolf von Laban. *Modern educational dance*. Princeton Book Co Pub, 1975. 1.1.3